

## THAI EASTERN ECONOMIC CORRIDOR DROUGHT MONITORING USING TERRA/MODIS SATELLITE-BASED DATA

Phaisarn JEEFOO<sup>1</sup> 

DOI: 10.21163/GT\_2023.182.09

### ABSTRACT:

One of the main natural disasters that has an impact on the environment and economy of nations throughout the world is drought. It has an impact on the local vegetation's state. The study's main goal was to look for years of severe drought by looking at Thailand's Eastern Economic Corridor (EEC). To determine the vegetation condition in the research area between 2017 and 2021, the Normalized Vegetation Index (NDVI) from Terra/MODIS data was employed. The area with the NDVI difference from the average value of NDVI during the same time period was examined using the Standardized Vegetation Index (SVI). Through the vegetation index, the drought can be reflected in this. According to the study, the highest drought area covered an area of 216.36 km<sup>2</sup> in 2017. This was followed by years 2019 and 2020, which each covered an area of 212.65 km<sup>2</sup>, 211.23 km<sup>2</sup>, 197.09 km<sup>2</sup>, and 178.07 km<sup>2</sup>. Additionally, a statistical analysis of the monthly correlation between the SVI (independent variable) and rainfall (dependent variable) over the course of the five years revealed that the coefficient of determination R<sup>2</sup> was 0.8018 in 2020, 0.6819 in 2021, 0.6262 in 2017, 0.5772 in 2018, and 0.5108 in 2019. The methodology can be obtained and used by other departments to assess and forecast drought in other regions of Thailand and other nations.

**Key-words:** Drought, Terra/MODIS, NDVI, SVI, Thai Eastern Economic Corridor.

### 1. INTRODUCTION

One of the worst weather-related catastrophes is drought. For drought management, accurate information about its length, spatial coverage, intensity, and impact is crucial. Especially in the agricultural sector, droughts frequently result in the loss of livelihoods along with various negative environmental effects (Willibroad & Sang-Il, 2019; Abbas et al., 2022). Identification of drought trends could be utilized as a strategy for monitoring and sustainable management because marshes and vegetation next to inland water bodies depend on the water supply within their ecosystem (Villarreal et al., 2016). A drought was a natural water shortage brought on by erratic and delayed rain. Devastated crops, starvation, conflicts, and wars are a few effects of drought (Su et al., 2017). When the demand for water exceeds the supply, a drought occurs. It is believed that among all dangers, natural disasters have the greatest effects on people (Qin et al., 2021). That had an impact on lifestyle and the global economic system, with emphasis on Thailand (Gomasathit et al., 2015). Therefore, it is crucial to consider rainfall while looking for relationships between it and the spectral index. Additionally, the correlation between rainfall and the spectral index is a key metric for identifying drought zones in order to analyze the length of rainfall that impacts vegetation (Rimkus et al., 2017). Rainfall was the primary source of the drought in Thailand, which had been an ongoing issue, particularly in the northern east and western south. Every year, there has been a lack of rain, especially from winter to summer (Thai Meteorological Department, 2021). Although drought is not a new problem, it recurs every year, particularly in the north and east of the country. Low precipitation levels, which frequently recur every cold season until hot season, are the main cause of drought. Water scarcity has an impact on vegetation phenology, which will then reveal the amount of drought severity (Laosuwan et al., 2016).

---

<sup>1</sup> Research Unit of Spatial Innovation Development (RUSID), Geographic Information Science, School of Information and Communication Technology, University of Phayao, Thailand, [phaisarn.je@up.ac.th](mailto:phaisarn.je@up.ac.th).

Modern and cutting-edge technology, remote sensing is particularly useful for predicting natural disasters including flooding, drought, sea level rise, changes in land use and cover, and so forth (Uttaruk & Laosuwan, 2017a). Remote sensing-based indices frequently make use of observations from a variety of spectral bands, each of which offers a unique perspective on the surface's state at various periods. Standardized Vegetation Index (SVI) and Normalized Vegetation Index (NDVI) are two remote sensing-based indicators (Rotjanakusol, T. & Laosuwan, 2018; Buma & Sang-II, 2019). Data from satellites that have undergone image processing and mathematical calculations will clearly show the study's specifics. For instance, the NDVI is determined by the variations in red and near-infrared wavelengths (Kaspersen et al., 2015; Ganie & Nusrath, 2016). To determine the state of the vegetation in the research area, NDVI from MODIS data was employed. The area with the NDVI difference from the average value of NDVI over the same time period was also examined using SVI. Through the vegetation index, the drought can be reflected in this. The study has used an analysis technique to determine how a drought develops through time and space. Effectively identifying the origin and type of drought was possible thanks to several satellite photos collected from MODIS data. The preparation of the drought mitigation in the area for the concerned agencies will benefit from this.

In addition, the SVI, which is based on calculations from 16-day NDVI data, represents the possibility of vegetation condition deviation from normal. The goal of this work was to standardize, by time of year, the NDVI to enhance drought-monitoring techniques. For the three provinces or Eastern Economic Corridor (EEC) of Thailand, the study used series of MOD13Q1 MODIS satellite pictures over a 5-year period (2017, 2018, 2019, 2020, and 2021), (Fig. 1).

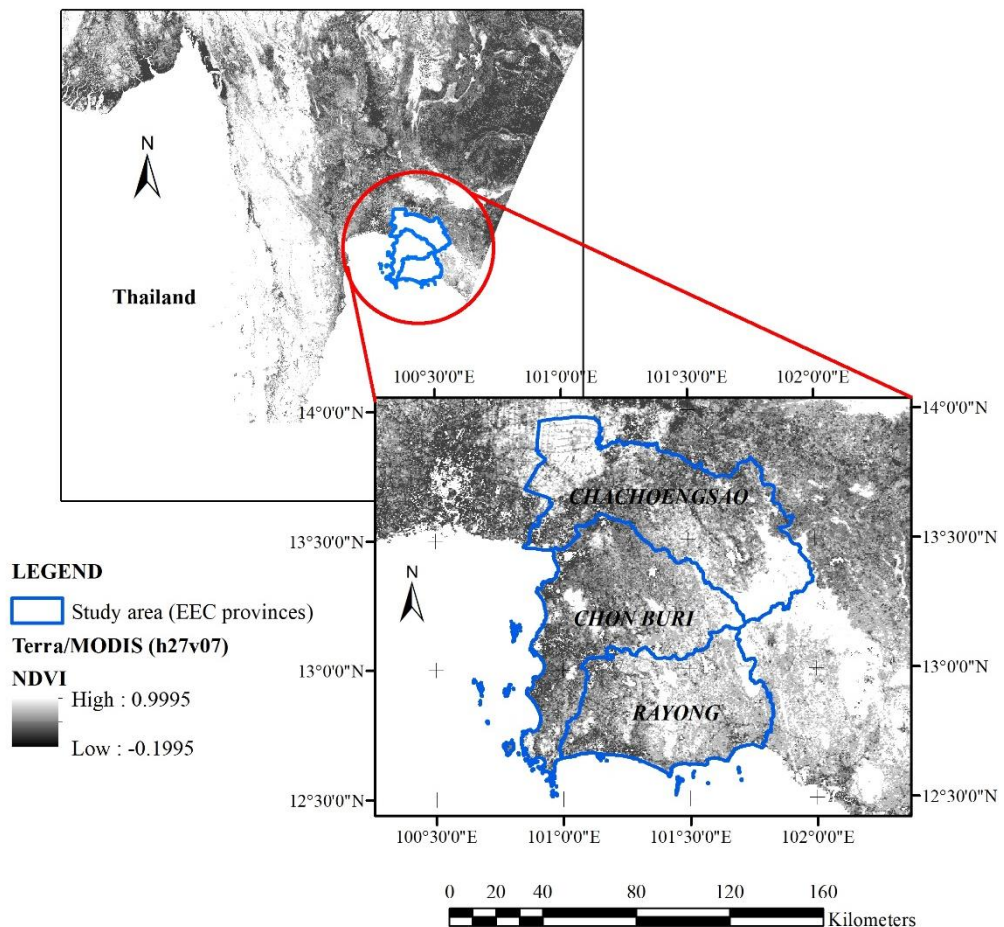


**Fig. 1.** The study area: Eastern Economic Corridor of Thailand (EEC).

## 2. STUDY AREA

The well-known Eastern Seaboard Development Program, which has supported Thailand as a driving force for industrial output in Thailand for more than 30 years, is being revitalized and enhanced as part of the Thailand 4.0 scheme's EEC development plan. The Eastern Economic Corridor Office of Thailand (the EECO) has been tasked with leading the nation's investment in advancing innovation and cutting-edge technology for the next generation under this program. Thailand's investment in the region's physical and social infrastructure will significantly advance and change under the direction of the EEC Development Plan. The first focus of the EEC project will be on three eastern provinces: Chachoengsao, Chonburi, and Rayong (**Fig. 1**). The EEC is 120 km east of Bangkok, and covers an area of 13,418 km<sup>2</sup> with geographical location between 12°30'0''N to 14°0'0''N and 100°30'0''E to 102°0'0''E. In terms of climate characteristics, the region experiences a tropical monsoon, with sea breezes blowing all year round. The temperature is moderately warm. Rainfall is heavy from May to October every year in the cool coastal regions during the rainy season. With an approximate elevation of 1,050 meters above mean sea level, it is primarily covered by mountainous terrain.

## 3. DATA AND METHODS

### 3.1. Data from Terra/MODIS satellite

Data on natural resources will be monitored and examined by the Terra/MODIS satellite. With a spatial resolution of 250 to 1,000 meters and 36 spectral bands, the sweep width is approximately 2,330 kilometers. Within two days, the Terra/MODIS satellite collects worldwide digital data. Terra/MODIS data (Buma & Sang-II, 2019) are therefore suitable for tracking spatial changes that are widespread. The MOD13Q1 product (h27v07), whose NDVI data sets covered the period from 2017 to 2021, was used in this study. Data collected in each month of the years 2017, 2018, 2019, 2020, and 2021 are used to create the MOD13Q1 data. WGS84-UTM zone 47N coordinates will be used for geometric adjustment. The closest neighbor method will be used to evaluate pixel locations, and a subset of satellite data will be created that solely includes the provinces of the EEC.

### 3.2. Data from rainfall and temperature

In order to establish the temporal association with the SVI mean, the average monthly rainfall data for the years 2017, 2018, 2019, 2020, and 2021 was used. For data collection, only Thai Meteorological Department (TMD) ground stations that monitor rainfall in the eastern region were utilized. Procedures of data analysis are determined in a logical order for analyzing drought in Rayong province (**Fig. 2**).

The vegetation condition in the study region has been determined using the NDVI acquired from the MODIS data. Additionally, the SVI was utilized to evaluate the region where the NDVI value differed from the NDVI average throughout the same time period. Through the vegetation index, the drought can be reflected in this. The study has used an analysis technique to determine how a drought develops through time and space. Effectively identifying the origin and type of drought was possible thanks to several satellite photos collected from MODIS data. The preparation of the drought mitigation in the area for the concerned agencies will benefit from this.

### 3.3. NDVI analysis

Equation 1 demonstrates that the electromagnetic reflection of RED wave and NIR wave were calculated differently.

$$NDVI = \frac{NIR-RED}{NIR+RED} \quad (1)$$

The NDVI readings ranged from -1 to +1. The NDVI displayed a negative result for the water area. The NDVI value for the land region with less vegetation was almost zero. A +1 was indicated for the green region. Because of these capabilities, NDVI was used as a tool to forecast and study changes in vegetation that were influenced by the environment (Laosuwan et al., 2016; Buma & Sang-II, 2019).

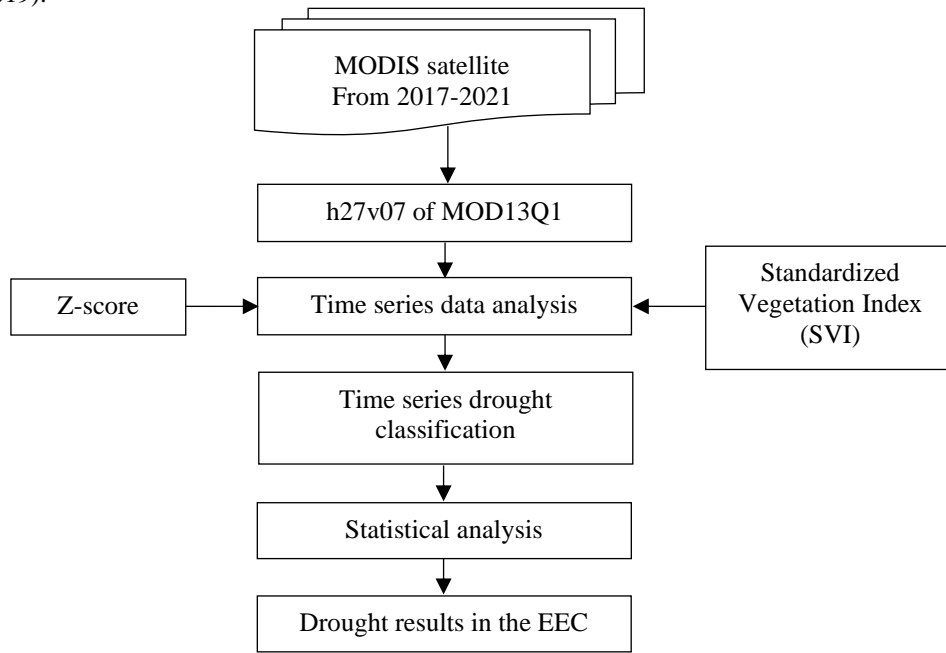


Fig. 2. Flowchart of methodology.

### 3.4. SVI analysis

The monthly MOD13Q1 (NDVI) data are utilized because the SVI value was derived from NDVI and because they can be a valuable indicator and are frequently used for monitoring and analyzing vegetation dynamics. The MOD13Q1 (NDVI) data's z-scores are used to calculate the SVI value for each pixel point. The standard score is generated using the NDVI of each pixel location for each season to determine the standard deviation from the mean in a unit of standard deviation. The three periods (seasons in Thailand) that make up this study's classification of the seasons are the summer (17 February to 16 May), the rainy season (17 May to 16 October), and the winter (17 October to 16 February). The specifics of the z-score analysis were shown in equation 2.

$$Z_{ijk} = \frac{NDVI_{ijk} - \overline{NDVI}_{ij}}{\sigma_{ij}} \quad (2)$$

where;

$Z_{ijk}$  = the z-value for pixel  $i$  during week  $j$  for year  $k$

$NDVI_{ijk}$  = the weekly NDVI value for pixel  $i$  during week  $j$  for year  $k$

$\overline{NDVI}_{ij}$  = the mean NDVI for pixel  $i$  during week  $j$  over  $n$  year and

$\sigma_{ij}$  = the standard deviation of pixel  $i$  during week  $j$  over  $n$  years

From the equation 2, the  $Z_{ijk}$  value is a hypothesis value to be consistent with a standard normal distribution with the mean of 0 and standard deviation of 1 to examine hypothesis from pixel locations in each season of the year 2017, 2018, 2019, 2020 and 2021. The probability value of  $SVI = P(Z_{ijk})$  of the standard score of NDVI to reflect the probability of plant conditions. The SVI analysis can be seen in the equation 3 (Uttaruk & Laosuwan, 2017a; Uttaruk & Laosuwan, 2019; Pachanaparn et al., 2022).

$$SVI = \frac{Z_{ijk} - Z_{ijMIN}}{Z_{ijMAX} - Z_{ijMIN}} \quad (3)$$

where;

$Z_{ijk}$  = z-value for pixel i during week j for year k;

$Z_{ijMAX}$  = maximum of z-value for pixel i during week j

$Z_{ijMIN}$  = minimum of z-value for pixel i during week j

From the Equation 3, the probability of each pixel location will be shown in SVI value to recognize the greenness of plants in different seasons or different periods. The study will conduct over the 5 years periods (2017-2021) to indicate comparison of high level and low level of drought observed in the mentioned periods based on the seasons. It is an estimation of probability of current vegetation condition from previous vegetation condition. SVI value would lie above zero but lower than one ( $0 < SVI < 1$ ) where 0 is the lowest standard score of NDVI value at a pixel location observed at a certain time of the 5 years period and 1 is the highest standard score of NDVI value at a pixel location observed at a certain time of the 5 years period.

### 3.5. Spatial analysis of drought

In each month of the years 2017, 2018, 2019, 2020, and 2021, the critical levels of vegetation were used to categorize the spatial study of drought intensity. There are 5 levels of SVI drought severity. **Table 1**, lists the five SVI drought levels, with the lowest level (0.00–0.05) denoting a very high drought and the highest level (0.9–1.00) denoting a very low drought.

**Table 1.**

**SVI level, percentage of SVI and drought level.**

Drought level of SVI	Percentage of SVI	Vegetation density
1.00 – 0.95	96.0% - 100%	Very high
0.95 – 0.75	76.0% - 95.0%	High
0.75 – 0.25	26.0% - 75.0%	Moderate
0.25 – 0.05	6.0% - 25.0%	Low
0.05 – 0.00	0% - 5.0%	Very low

### 3.6. Multi-temporal drought analysis

In this study, the average monthly rainfall data for the years 2017, 2018, 2019, 2020, and 2021 collected from TMD's rainfall measurement earth station, a total of 28 stations covering only the study area, will be analyzed with the SVI analysis results.

### 3.7. Statistic correlation analysis

The results of the SVI analysis and the rainfall data for the years 2017, 2018, 2019, 2020, and 2021 are shown to explain how the linear regression analysis technique was used to rectify the statistical errors. The SVI index was used to display the probabilities in the photos. Using the vegetation state from the pass, it was possible to estimate the likelihood of the current vegetation. The SVI values ranged from greater than zero to less than one ( $0 < SVI < 1$ ). The lowest standard SVI score from photos taken in 2017 through 2021 was zero.

### 3.8. SVI Analysis for Drought Monitoring

The standard scores used for the SVI computation were derived using monthly SVI data for the years 2017, 2018, 2019, 2020, and 2021. The average and standard deviation for each image then needed to be determined. The standard scores for each month and year were needed for the SVI calculation, which was followed by an analysis for monthly likelihood in each image's point. By categorizing SVI values into levels, the monthly SVI maps for the years 2017, 2018, 2019, 2020, and 2021 were created.

## 4. RESULTS AND DISCUSSIONS

### 4.1. SVI analysis results

The SVI was used to track droughts by analyzing reflections of vegetation probabilities throughout a variety of time periods. Calculations were made of the SVI variations at each point and time period in each year. The findings showed that in 2017, the vegetation density ranged from 0 to 1, with the lowest, greatest, average, and standard deviation of SVI representing it.

In each season and time period, the average represented vegetation density and drought. The lowest average was 0.1252 in February, the previous winter season, and the highest average was 0.1484 in October (16/10/2017), the rainy season. In 2018, the winter season's highest average was 0.1467 while the early wet season's lowest average was 0.1140. The lowest average was 0.1262 in August during the rainy season, and the highest average in 2019 was 0.1429 in November (01/11/2019).

The winter season's highest average in 2020 was 0.2053 in December, while the winter season's lowest average was 0.1269 in February. In 2021, the early rainy season's May had the greatest average of 0.2101 and the winter season's January had the lowest average of 0.1231. The averages, SVI standard deviation, and the lowest and highest standard scores all played a role in determining the SVI variances for each season and time period. Therefore, the fifth year SVI averages could be concluded (**Fig. 3**).

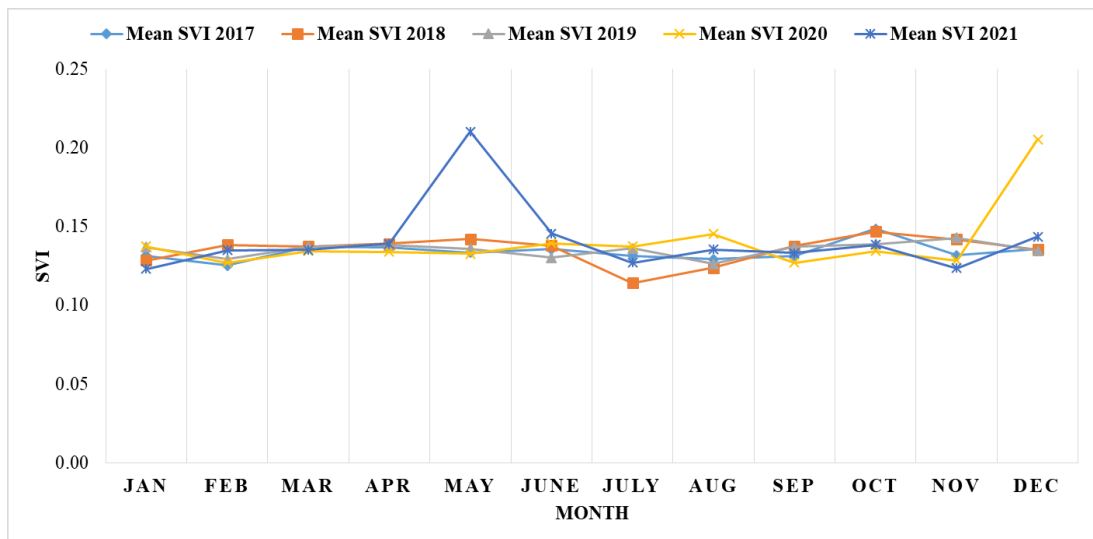


**Fig. 3.** Fifth year SVI averages.

The SVI variations in each period and season, which were influenced by vegetation density and rainfall, were depicted by the graphs. Results were poor from January through April during the heat. The lowest result was obtained in July 2018, and it rose to the highest level during the winter months of December 2020 and early rainy season in May 2021. Early in the winter, in October, it had begun to decline once more.

Additionally, this study's analysis of the yearly SVI included data from monthly data overlays, which allowed it to more accurately depict the spatial and temporal nature of droughts than monthly data alone. In **Fig. 4**, the year 2021 had the worst spatial drought, which was followed by the years 2018, 2020, 2019, and 2017 in that order.

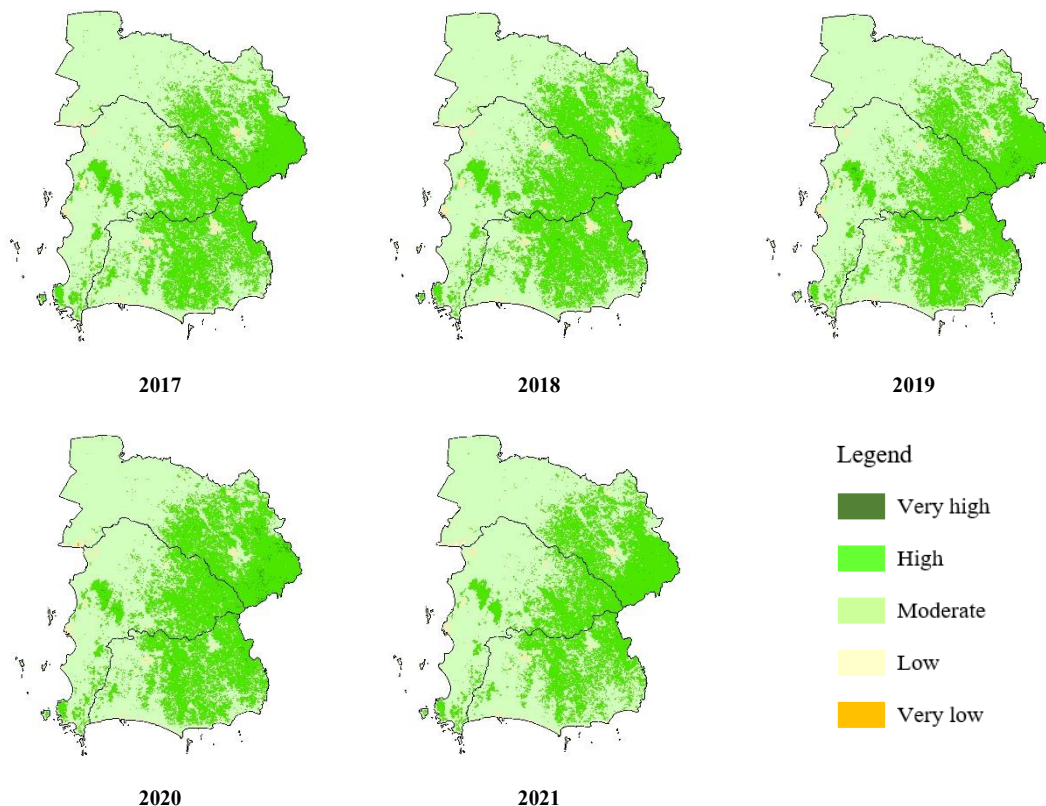


Fig. 4. SVI yearly analysis from 2017 - 2021.

#### 4.2. Multi-Temporal analysis results

SVI monthly average and rainfall during a five-year period revealed that the SVI average's temporal variation matched the monthly rainfall; however, the change in SVI was slower than that of rainfall because vegetation only began to grow after receiving enough water for leaf formation or growth. The summary of the multitemporal drought analysis is shown in Fig 5

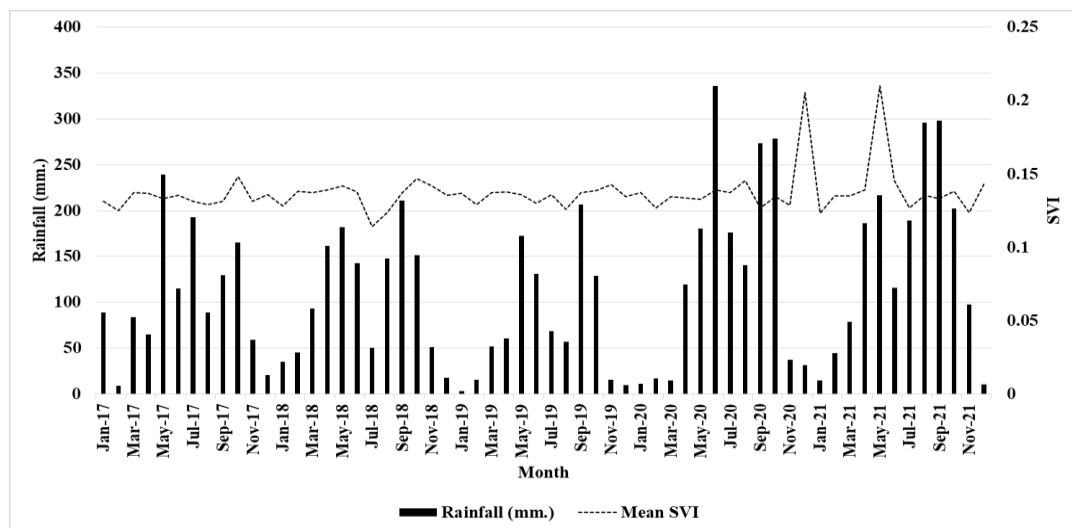


Fig. 5. Multi-temporal drought analysis.

In 2017, variations in rainfall were lowest from January to April, peaked in May, and then fell to their lowest level in October. In 2018 and 2019, variations in rainfall were lowest in January, climbed steadily, peaked in May, dropped to their lowest in July, peaked again in September, and finally decreased to their lowest in December. Rainfall variations in 2020 and 2021 were somewhat greater in January and then decreased until May, grew steadily and peaked in June, September, and October, and then steadily decreased and reached their lowest point in December.

### 4.3. Statistical correlation analysis results

The outcome of a statistical correlation analysis between SVI (the independent variable) and rainfall (the dependent variable) from 2017 to 2021 revealed a correlation between the two variables. The correlation equation for SVI and rainfall in 2020 is given by the statistical correlation analysis, and it is given by  $y = 1623.1 \times -148.31$ , with an  $R^2$  coefficient of determination of 0.8018. The correlation equation for SVI and rainfall in 2021 was determined to be  $y = 2107.5 \times -181.96$  and the coefficient of determination  $R^2$  was found to be 0.6819. SVI and rainfall data from 2017 were statistically correlated, and the correlation equation was given as  $y = 8745.2 \times -1096.6$  with an  $R^2$  coefficient of determination of 0.6262. A correlation equation of  $y = 6419.8 \times -758.51$  and a coefficient of determination of  $R^2 = 0.5772$  were produced by the statistical correlation analysis results between SVI and rainfall in 2018. A correlation equation of  $y = 12103 \times -1544.7$  and a coefficient of determination  $R^2 = 0.5108$  were obtained by the most recent statistical investigation of the relationship between SVI and rainfall in 2019 (Table 2).

**Table 2.**  
**Statistical correlation analysis from 2017 – 2021.**

Year	Correlation equation	$R^2$
2017	$y = 8745.2x - 1096.6$	0.6262
2018	$y = 6419.8x - 758.51$	0.5772
2019	$y = 12103x - 1544.7$	0.5108
2020	$y = 1623.1x - 148.31$	0.8018
2021	$y = 2107.5x - 181.96$	0.6819

## 5. CONCLUSIONS

The average SVI could be employed as a comparison operator in this study. Drought was implied by low SVI levels, and the closer to zero the value was, the worse the drought. High SVI, however, indicated abundance; the closer to 1, the greater the abundance and absence of drought. The study also discovered that the largest drought area was in 2017, covering an area of 216.36 km<sup>2</sup>, followed by 2019 (212.65 km<sup>2</sup>), 2021 (211.23 km<sup>2</sup>), 2020 (197.09 km<sup>2</sup>), and 2018 (178.07 km<sup>2</sup>), respectively. Results of a multitemporal drought analysis between SVI and rainfall revealed that during the course of the five-year study period, the monthly averages of SVI and rainfall were consistent with one another, as depicted in the typical graph in Fig. 5. SVI increased in response to increasing rainfall, and declined in response to decreasing rainfall. However, because vegetation only began to grow once enough water was available for leaf formation or growth, the change in SVI was slower than the rise in rainfall. The coefficients of determination ( $R^2$ ) for the correlation between SVI and rainfall over the 5 years (2017 to 2021) were found to be 0.8018, 0.6819, 0.6262, 0.5772, and 0.5108, respectively. The findings of this study align with those of similar research on drought analysis using satellite-based data and spectral indices, such as studies conducted in upper northeastern Thailand and Mahasarakham province (Laosuwan et al., 2016; Rotjanakusol, & Laosuwan, 2018), drought detection by application of remote sensing technology and vegetation phenology (Uttaruk & Laosuwan, 2017b). The SVI is a helpful instrument that can provide information about the onset, scope, intensity, and duration of vegetative stress in close to real-time (Sruthi & Mohammed Aslam, 2015; Vicente-Serrane et al., 2015; Pachanaparn et al., 2022). The findings of this study offer a standard for accurately identifying the drought region in the EEC provinces of Chachoengsao, Chonburi, and Rayong. Additionally, the appraisal of the drought area will be reliable and reasonably quick. The methodology can be obtained and used by other departments to assess and forecast drought in other regions of Thailand and other nations.



## ARCKNOWLEDGEMENT

I wish to acknowledge funding from the United Nations Development Programme (UNDP), which supports a project through the Climate Change Modelling in coastal zones in the Gulf of Thailand. I acknowledge the School of Information and Communication Technology (ICT), University of Phayao Thailand for providing the available facilities to carry out this research.

## REFERENCES

- Abbas, A., Huang, P., Hussain, S., Shen, F., Wang, H. & Du, D. (2022) Mild Evidence for Local Adaptation of *Solidago Canadensis* under Different Salinity, Drought, and Abscisic Acid Conditions. *Polish Journal of Environmental Studies*, 31(4), 2987-2995.
- Buma, W.G. & Sang-II, L. (2019) Multispectral Image-Based Estimation of Drought Patterns and Intensity around Lake Chad, Africa. *Remote Sensing*, 11(2534), 1-21.
- Ganie, M.A. & Nusrath, A. (2016) Determining the Vegetation Indices (NDVI) from Landsat 8 Satellite Data. *International Journal of Advanced Research*, 4(8), 1459-1463.
- Gomasathit, T., Laosuwan, T., Sangpradid, S. & Rotjanakusol, T. (2015) Assessment of Drought Risk Area in Thung Kula Rong Hai using Geographic Information System and Analytical Hierarchy Process. *International Journal of Geoinformatics*, 11(2), 21-27.
- Kaspersen, P.S., Fensholt, R. & Drews, A. (2015) Using landsat Vegetation Indices to Estimate Impervious Surface Fractions for European Cities. *Remote Sensing*, 7, 8224-8249.
- Laosuwan, T., Sangpradid, S., Gomasathit, T. & Rotjanakusol, T. (2016) Application of remote Sensing Technology for Drought Monitoring in Mahasarakham Province, Thailand. *International Journal of Geoinformatics*, 12(3), 17-25.
- Pachanaparn, C., Jeefoo, P. & Rojanavasuu, P. (2022) Application of Remote Sensing for Drought Monitoring with NDVI-based Standardized Vegetation Index in nan Province, Thailand. The 7th International Conference on Digital Arts, Media and Technology (DAMT) and 5th ECTI Northern Section Conference on Electrical, Electronics, Computer and Telecommunications Engineering (NCON), pp. 330-335, Chiang Rai, Thailand, 26-28 January 2022.
- Qin, Q. Wu, Z. Zhang, T. Sagan, V., Zhang, Z., Zhang, Y., Zhang, C., Ren, H., Sun, Y., Xu, W. & Zhao, C. (2021) Optical and Thermal Remote Sensing for Monitoring Agricultural Drought. *Remote Sensing*, 13(5092), 1-34.
- Rimkus, E., Stonevicius, E., Kipys, J., Maciulyte, V. & Valiukas, D. (2017) Drought Identification in the Eastern Baltic Region using NDVI. *Earth System Dynamics*, 8(3), 627-637.
- Rotjanakusol, T. & Laosuwan, T. (2018) Remote Sensing Based Drought Monitoring in the Middle-Part of Northeast Region of Thailand. *Studia University*, 28(1), 14-21.
- Sruthi, S. & Mohammed Aslam, M.A. (2015) Agriculture Drought Analysis Using the NDVI and Land Surface Temperature Data; a Case Study of Raichur District. *Aquatic Procedia*, 4, 1258-1264.
- Su, Z., He, Y., Dong, X. & Wang, L. (2017) Chapter 8: Drought Monitoring and Assessment using Remote Sensing. *Springer International Publishing Switzerland, V. Lakshmi (ed.), Remote Sensing of Hydrological Extremes, Springer Remote Sensing/Photogrammetry*, 151-172.
- Thai Meteorological Department, (2021) The Expectation of the Weather during the Rainy Season of 2013. Available online: <http://www.tmd.go.th> (accessed on 11 October 2021).
- Uttaruk, Y. & Laosuwan, T. (2017a) Carbon Sequestration Assessment of the Orchards using Satellite Data. *Journal of Ecological Engineering*, 18(1), 11-17.
- Uttaruk, Y. & Laosuwan, T. (2017b) Drought detection by application of Remote Sensing technology and vegetation phenology. *Journal of Ecology Engineering*, 18(6), 115-121.
- Uttaruk, Y. & Laosuwan, T. (2019) Drought analysis using satellite-based data and spectral index in upper northeastern Thailand. *Polish Journal of Environmental Studies*, 28(6), 4447-4454.
- Vicente-Serrane, S.M., Cabello, D., Tomas-Burguera, M., Martin-Hernandez, N., Beegueria, S., Azorin-Molina, C. & Kenawy, A.E. (2015) Drought Variability and Land Degradation in Semiarid Regions: Assessment Using Remote Sensing Data and Drought Indices (1982-2011). *Remote Sensing*, 7, 4391-4423.
- Villarreal, M.L., Norman, L.M., Buckley, S., Wallace, C.S.A. & Coe, M.A. (2016) Multi-index time series monitoring of drought and fire effects on desert grasslands. *Remote Sensing of Environment*, 183, 186-197.
- Willibroad, G.B. & Sang-II, L. (2019) Multispectral Image-Based Estimation of Drought Patterns and Intensity around Lake Chad, Africa. *Remote Sensing*, 11, 1-21.